Assessment of the Use of Lightning Information in Satellite Infrared Rainfall Estimation

MIRCEA GRECU AND EMMANOUIL N. ANAGNOSTOU

Department of Civil and Environmental Engineering, University of Connecticut, Storrs, Connecticut

ROBERT F. ADLER

Laboratory for Atmospheres, NASA Goddard Space Flight Center, Greenbelt, Maryland

(Manuscript received 22 October 1999, in final form 18 February 2000)

ABSTRACT

In this paper, the combined use of cloud-to-ground lightning and satellite infrared (IR) data for rainfall estimation is investigated. Based on analysis of the correlation between satellite microwave and IR rainfall estimates and on the number of strikes in ''contiguous'' areas with lightning, where the contiguity is defined as a function of the distance between strikes, an empirical algorithm is developed for convective rainfall estimation. The rainfall in areas not associated with lightning is determined using a modified version of an existing IR-based rainfall estimation technique. The combined lightning and IR-based technique is evaluated based on 15 days of data in July 1997 provided by geostationary and polar-orbiting satellites and the National Lightning Detection Network. The general conclusion is that lightning data contain useful information for IR rainfall estimation. Results show a reduction of about 15% in the root-mean-square error of the estimates of rain volumes defined by convective areas associated with lightning. It is shown that the benefit of using lightning information extends to the whole rain domain, because the error caused by missing convective areas because of the absence of lightning is smaller than that caused by overestimating the convective rain areas because of cirrus that obscure underlying convective storms when only satellite IR data are used.

1. Introduction

Accurate rainfall estimation is an essential condition for the success of numerous scientific and practical applications in areas such as climatology, hydrology, water resources, and agriculture. Although weather radars (and rain gauges) can provide rainfall estimates of appropriate accuracy for some of these applications, they cannot represent the general solution to the problem because of the existence of large remote areas not covered by these sensors (mountains, tropical rain forests, etc). For such areas, alternative sources of rain estimates are needed. In this respect, meteorological satellite observations can be a solution, despite various issues that are yet to be resolved. Active and passive microwave sensors aboard polar-orbiting satellites provide observations physically connected to precipitation but at a temporal resolution (once or twice a day) that considerably limits their utility in many applications. In these conditions, the cloud-top infrared (IR) observations from geostationary satellites remain the main data source for near-continuous monitoring from space.

The main difficulty in IR-based rainfall estimation is the fact that precipitation can only be inferred from cloud-top observations. Because a cloud's brightness temperature, or other cloud-top characteristics, may correspond to different surface rainfall rates depending on the rain regime or other factors, IR-based rainfall estimation may be improved significantly only by considering additional information. Past studies (Adler and Negri 1988; Anagnostou et al. 1999) have shown that minima in the IR temperature array may be associated with enhanced convective regions in the cloud, and substantially better estimates may be obtained by using distinct algorithms for convective and stratiform precipitation. The ability to detect convective cores and rain/no-rain boundaries, however, is limited from only being able to ''see'' the features at cloud top. Thus, the quantification of the convective rainfall is subject to significant uncertainty, despite the fine time resolution of the data. To reduce this uncertainty, additional information should be considered. Lightning data may represent such information.

The association of lightning with convective precipitation has been addressed in an early study by Goodman

Corresponding author address: Emmanouil N. Anagnostou, Department of Civil and Environmental Engineering, University of Connecticut, 261 Glenbrook Rd., Storrs, CT 06269.
E-mail: manos@engr.uconn.edu

(1990), who related lightning occurrence to convective activity, and in later studies (Zipser 1994; Petersen and Rutledge 1998; Toracinta et al. 1996; Cheze and Sauvageot 1997, among others) that demonstrated more-quantitative relationships between lightning discharges and other measurables of rainfall. It thus is expected that incorporation of lightning information into an IR retrieval scheme would allow better estimation of the convective rain area and volume.

The idea of using lightning data for rainfall estimation is not new. Among the latest approaches are those of Sheridan et al. (1997), Cheze and Sauvageot (1997), Tappia et al. (1998), Morales et al. (1998), and Alexander et al. (1999). Sheridan et al. (1997) investigated relationships between large-area (on the order of 10 000 km^2) daily accumulations and corresponding lightning observations. Cheze and Sauvageot (1997) developed relationships for characterizing the rainfall volume as a function of lightning activity for areas on the order of 40 000 km^2 and 15-min accumulations. Petersen and Rutledge (1998) analyzed the relation between cloud-to-ground lightning and convective rainfall and evaluated its dependence on the type of convection. Tappia et al. (1998) proposed a model for 25π km^2 and 5-min-resolution rainfall estimation. Morales et al. (1998) used data from an experimental very low–frequency radio receiver network, implemented by the National Aeronautics and Space Administration and Resolution Displays, Inc., to monitor lighting activity at long ranges, in conjunction with IR imagery to generate continuous estimates of rainfall over North America and northern South America. In this study, we consider lightning as complementary information to a satellite IR convective–stratiform rainfall estimation technique (Adler and Negri 1988). Specifically, we utilize the lightning information to help to deduce the convective portion of the rainfall. We demonstrate that a technique that considers both IR and lightning data is superior to a technique that uses only the IR data.

The research focuses on issues related to the improvement of convective rainfall estimation from IR with the use of lightning data. An attempt is made to address fundamental questions concerning the improvement feasibility, significance, and dependence on rainfall magnitude and scale of aggregation. This attempt is implemented through the development of a technique designed to produce instantaneous convective and stratiform rain-rate maps based on combining geosynchronous satellite IR (10.5–12.6-μm channel) and ground-based lightning data. The resolution of the retrieved rainfall maps is 12-km^2 grids. The new algorithm performance is evaluated in relation to the performance of the IR-only convective/stratiform technique (CST) of Adler and Negri (1988). The reference rainfall data source is derived from the Goddard Profiling (GPROF) algorithm (Kummerow et al. 1996) applied to Special Sensor Microwave Imager (SSM/I) data from collocated Defense Meteorological Satellite Platform (DMSP) overpasses.

The paper is organized as follows. The matched satellite and ground-based lightning datasets are described and analyzed qualitatively in section 2. Section 3 contains the description of the proposed rainfall estimation algorithm. A quantitative assessment of the algorithm is provided in section 4. The algorithm intercomparison results are described in section 5, and conclusions are presented in section 6.

2. Data analysis

The data used in this study consist of 15 days (13 to 28 July 1997) of Geostationary Operational Environmental Satellite (GOES) IR, SSM/I, and ground-based lightning observations within an area ranging from 25° to 38°N latitude and from 115° to 80°W longitude. The reference convective and stratiform rainfall rates were derived from SSM/I data using GPROF. Past studies indicated some problems in microwave rainfall retrieval. These problems include the high sensitivity of the retrieval over continental regions with respect to the 85-GHz channel observations (Conner and Petty 1998) and sampling and modeling errors (Kummerow 1998). Despite these problems, we consider the microwave-derived estimates to be a reasonable alternative to radar rainfall for comparison with the IR/lightning rain estimates. These comparisons also may be applied to remote areas (e.g., rain forests and oceans) where radar measurements are not available to calibrate IR and lightning-based rain estimates (Anagnostou et al. 1999). Microwave data from SSM/I sensors aboard the *F-10*, *F-13*, and *F-14* DMSPs were utilized in this study. The GPROF (SSM/I) rainfall estimates were projected on a 12-km resolution grid. A classification scheme developed by Anagnostou and Kummerow (1997) was applied to identify the convective and stratiform precipitation regions in the GPROF rainfall estimates. The histograms of convective and stratiform precipitation, constructed using all samples from the study period, are shown in Fig. 1. An objective methodology for evaluating the classification results from this current database is impossible in the absence of volume-scanning radar measurements. Nevertheless, the validity of this technique was demonstrated by Anagnostou and Kummerow (1997) based on comparisons with ground-based radar classification products such as those of Steiner et al. (1995). The lightning data originated from the National Lightning Detection Network (NLDN). NLDN provides information only on cloud-to-ground strikes but with high accuracy with respect to strike location because of its dense network. The IR observations were available at approximately 15-min time intervals and at a resolution of 4 km from the *GOES-8* satellite.

As a first step, we qualitatively analyzed the agreement between the data. The SSM/I-based precipitation classification for two cases is given in Fig. 2. For the

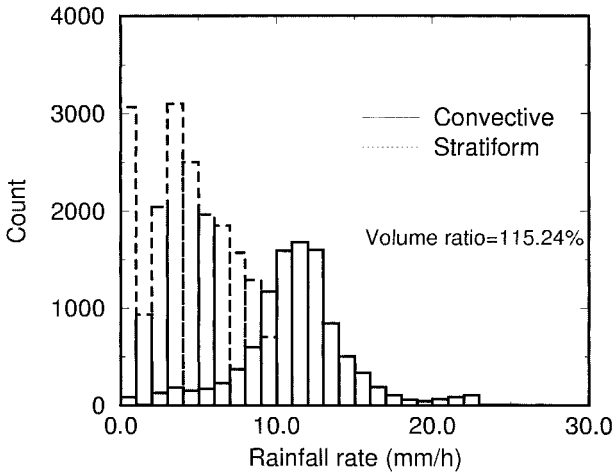

FIG. 1. Histogram of SSM/I convective and stratiform rainfall rates. Volume ratio is defined as the fraction of convective rain volumes relative to stratiform rain volumes.

same times, we plot the isotherms of 235-K IR brightness temperatures to indicate approximate cloud boundaries, the convective areas indicated by CST, and the lightning locations within a 15-min time window centered around the times of the SSM/I observations. Notice that there is fairly good agreement between the SSM/I and IR convective rain areas and the strike locations. There are situations of convective rain not associated with lightning, however, such as those over New Mexico in the top-right panel of Fig. 2. At this point, we note that NLDN picks up only cloud-to-ground strokes. Intracloud and cloud-to-cloud strokes may be five times as abundant as cloud–ground, and NLDN misses them (Mackerras et al. 1988). Such situations also have been noticed in other studies (Maddox et al. 1997). There also are situations in which CST fails to identify convective rain areas that are indicated by lightning and SSM/I (top-right panel in northern Mexico and southern New Mexico–Texas border). The cases presented herein provide an indication of the utility of lightning as a complementary data source in IR-based convective rainfall estimation. Another indication of the utility of the lightning information is the lack of cloud–ground lightning in locations of CST convective features (e.g., on the Texas and Oklahoma border). These IR convective features that do not appear in either the lightning or microwave data probably are not real and would be eliminated by use of the lighting information.

Another observation from Fig. 2 is a relative displacement between the lightning locations and SSM/I or IR convective areas. We consider this displacement to be a consequence of both the top outflow in a cloud that causes a displacement of the minimum temperature relative to the convective cores and possible spatial and temporal mismatches in the data. Figure 3 contains the histogram of SSM/I rainfall conditional on lightning occurrences. One can observe a large frequency of lightning locations characterized by zero rain at the time of SSM/I overpass, but the lightning can start as late as 7.5 min later or quit 7.5 min earlier. This result is due to errors in GPROF rainfall retrieval, spatial and temporal mismatches, and the fact that there may be nonrainy clouds with lightning. As the rainfall rate increases, there is an increasing percentage of the area associated with lightning. Low-intensity rainfall may be considered to originate from stratiform systems and would not be expected to have significant lightning [e.g., about 6% according to MacGorman and Morgenstern (1998)]. Even at rain rates greater than 10–12 mm h^{-1}, which usually are considered convective at this scale (Steiner et al. 1995), there is a significant amount of area with no lightning, however. This lack is due primarily to the convective rain areas surrounding the areas of lightning strikes and possible convective clouds with no cloud–ground lightning (e.g., warm rain processes).

3. Considerations for infrared and lightning rainfall estimation

In this section, we describe a quantitative analysis made to determine the worth of using lightning in combination with IR data for rainfall estimation. Negri and Adler (1993), who analyzed the skills and drawbacks of CST and other IR techniques, concluded that cirrus–thunderstorm and convective–stratiform discriminations have a large effect on the accuracy of rainfall estimation. Accordingly, we use lightning information to determine the convective rain areas, and the rain-rate estimation for these areas is based on both lightning and IR data. A detailed description of the newly developed convective–stratiform IR–lightning algorithm (CSIRL) is given below.

The qualitative analysis presented in the previous section suggests that there is a minimum spatial scale below which spatial and temporal discrepancies can affect the results considerably. We chose to aggregate the GPROF (SSM/I) and CST rain estimates to variable-size clusters defined by lightning occurrences. For example, two 12-km pixels with lightning would belong to the same cluster if they were neighboring or connected by other lightning pixels. The clusters were defined for each instantaneous SSM/I overpass matched with the IR and lightning data. We identified a total of 2183 lightning clusters with sizes varying from 288 to 22 176 km^2. We calculated, for each cluster, 1) the number of strikes that occurred within a 15-min interval centered on the SSM/I observation time, 2) the SSM/I-based (GPROF) rain volume, and 3) the IR-based (CST) rain volume. We chose 15 min as the lightning accumulation interval because SSM/I and IR observations are not always simultaneous, and the time lag between these two observations may not exceed 15 min (i.e., the IR time resolution). In any case, with the current data it is difficult to assess the optimal time window. Nevertheless, time series of IR and lightning frequencies, presented by

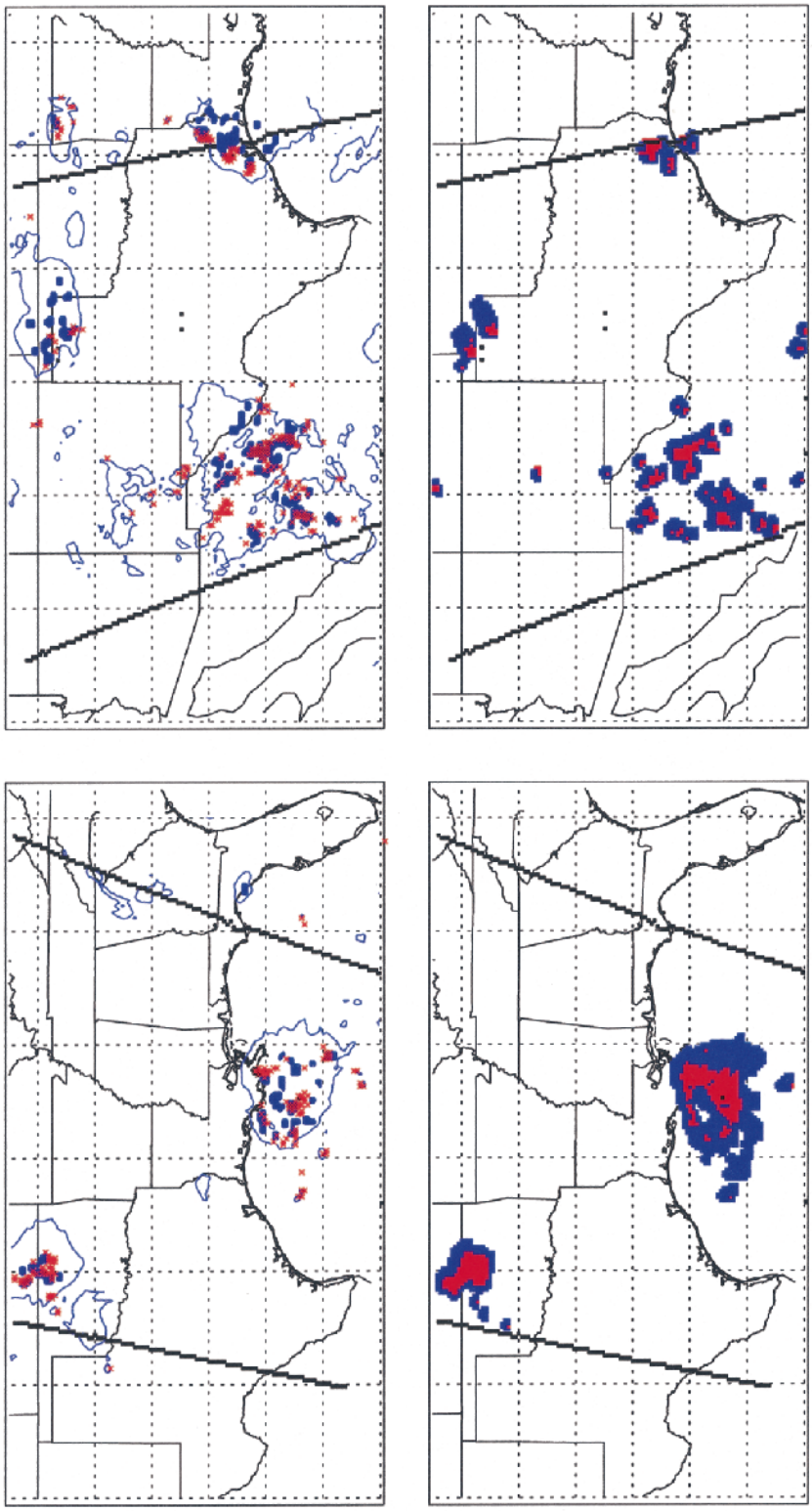

FIG. 2. Top panels: 235-K IR isotherms, CST convective areas (blue areas), and lightning locations (red crosses). Bottom panels: SSM/I-based convective (red) and stratiform (blue) rain areas. Right panels: 15 Jul 0014 UTC. Left panels: 17 July 1217 UTC.

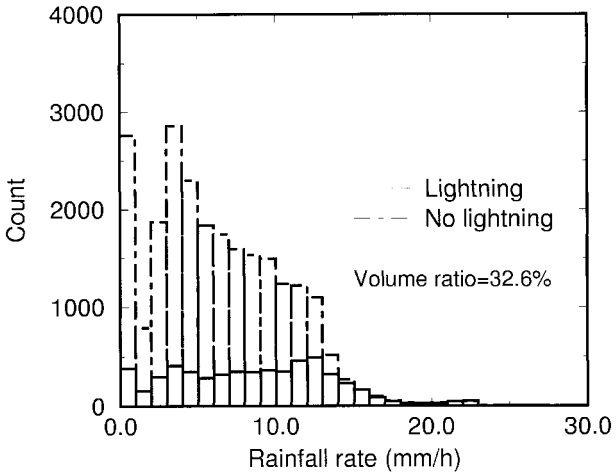

FIG. 3. Histogram of GPROF (SSM/I) rainfall rates associated with lightning. Volume ratio is defined as the fraction of rain volumes associated with lightning relative to those not associated with lightning.

Goodman et al. (1988), did not show any problem in using a 15-min time window for lightning accumulation.

The representation of SSM/I rain volume against the CST rain volume (lower panel) and the total number of strikes (upper panel) is shown in Fig. 4. Notice the similarity between the two panels of the figure. It may be that lightning information and IR-based rain retrievals (CST) have very similar correlations with rainfall derived from SSM/I data in areas that have lightning strikes. Note also that the correlation increases with the cluster's rain volume. To characterize this behavior numerically, we calculated the correlation conditionally on the clusters' rain volume (defined as the integral of the rainfall rate over an area) for several thresholds. In addition, we calculated the contributions of cluster rain volumes exceeding various thresholds to the total rain volume. Figure 5 shows the conditional correlations and rain fractions plotted against the selected threshold values. This figure gives a clear picture of the correlation dependence on the rain volume and the fraction of accumulated rain that corresponds to that correlation. This picture indicates that there is a serious limitation in collocating observations of small-scale rain systems from different remote sensors. Nevertheless, for the cases examined in this study, these systems contribute little to the overall rain volume. Therefore, it is better to consider the analysis at larger scales.

To determine a quantitative relationship for rain estimation using the data of the defined clusters, we employed a simple bivariate linear regression for the cluster's rain volume:

$$R = (a_0 + a_1 S/A + a_2 T)A, \qquad (1)$$

where R (mm h^{-1} km^2) is the cluster's rain volume, S is the number of strikes, T (K) is the minimum IR temperature in the cluster, and A is the number of 12-km

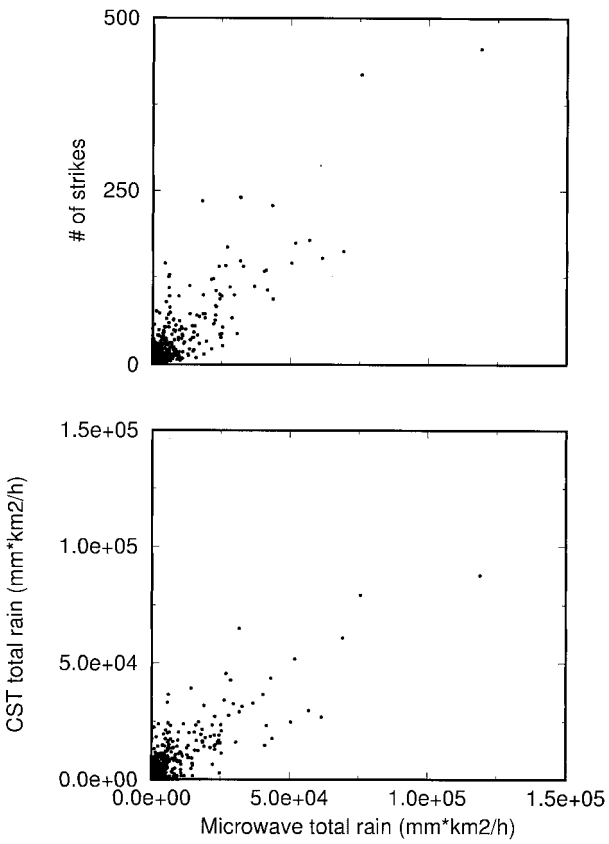

FIG. 4. Number of strikes (top panel) and CST rain volume (bottom panel) vs GPROF (SSM/I) rain volume for clusters defined by lightning occurrences.

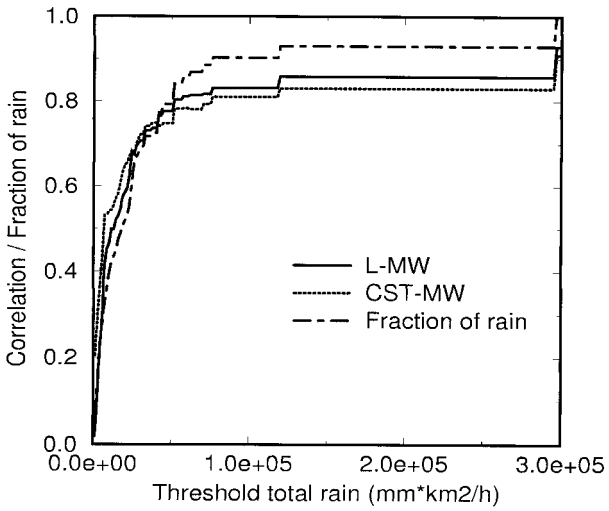

FIG. 5. Correlation between number of strikes and GPROF (SSM/I) rain volume for lightning clusters conditional on the rain volume magnitude.

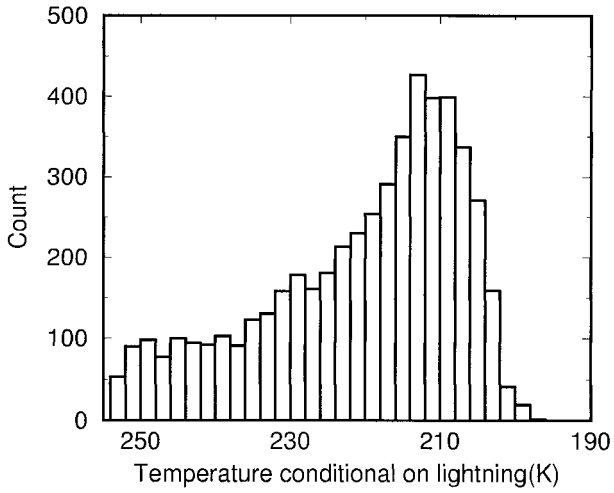

FIG. 6. Histogram of IR brightness temperatures at lightning locations.

pixels in the cluster. The coefficients a_0, a_1, and a_2 are determined using a least squares regression. The estimated parameter values and their significance are described in the next section.

A procedure is used for disaggregating the cluster's rain volume to its individual 12-km pixels. For this purpose, we use the histogram of the IR temperature, constructed from all pixels associated with lightning that exist in the dataset. The histogram is shown in Fig. 6. Based on that histogram, the following probabilities were calculated:

$$P(T_i) = P(\text{a raining pixel has temperature} \geq T_i). \quad (2)$$

The disaggregation procedure uses these IR temperature probabilities to compute weights for each individual 12-km pixel of a convective cluster. A pixel's weight is defined as the ratio of the pixel's probability to the sum of probabilities of all pixels located within the same convective cluster. The proposed combined IR–lightning algorithm for convective rainfall estimation can be summarized as follows:

1) read an IR observation array;
2) determine the lightning strikes within a 15-min window, centered around the IR sampling time;
3) determine the lightning clusters;
4) use (1) to determine the rain volume of each cluster; and
5) allocate the rain volume of each cluster to 12-km-resolution pixels based on (2).

The CSIRL procedure presented above estimates only the convective portion of the storm total precipitation. In the subsequent sections, we assess this new parameterization scheme for convective rainfall estimation and demonstrate improvements with respect to using solely IR or lightning data.

4. Assessment of CSIRL parameterization for convective rainfall estimation

Given that the size of the dataset available for calibration and validation of the CSIRL convective parameterization scheme is relatively small (i.e., 2183 lightning clusters), we devised a so-called randomization procedure (Noreen 1989) to test the significance of the performance of the parameterization scheme. The dataset was separated repeatedly into two subsets. One subset was used to estimate the parameters (a_0, a_1, and a_2) and the other to assess the performance of the calibrated algorithm [i.e., (1)]. The calibration–validation scenario was repeated several times and the mean and standard deviation of the algorithm error were determined. Error was defined as the difference between estimated and SSM/I-derived (GPROF) rain volume, integrated over the lightning-based defined convective clusters. As mentioned above, the size of these clusters varied from 288 to 22 176 km^2. Two error statistics were used: the root-mean-square error (rmse) and the differential bias. These statistics were normalized by the reference GPROF rain volume of the defined convective clusters. The calibration–validation methodology is formulated as following. Denoting N (2183) as the total number of defined convective clusters, n as the number of clusters used for calibration, and M ($\sim$1000) as the number of times the calibration–validation exercise was repeated, the steps of the randomization test procedure are as follows:

1) randomly select n out of N clusters;
2) regress for a_0, a_1, and a_2 parameters using the selected n clusters;
3) calculate the error statistics in the remaining $N - n$ clusters;
4) repeat the first three steps M times; and
5) change n and repeat (n is varied five times).

The mean values of parameters identified by this calibration–validation exercise are $a_0 = 31.23$, $a_1 = 0.1385$, and $a_2 = -0.1311$. The results yielded by the validation are shown in Fig. 7. Four algorithms are compared in this figure: CST applied on IR-only data; CSIRL [(1)] applied on both IR and lightning data; and two other versions of CSIRL, one with $a_1 = 0$ (uses only IR data) and the second with $a_2 = 0$ (uses only lightning data). The CST algorithm was used with the original parameters presented in Adler and Negri (1988). The conclusions drawn by analyzing Fig. 7 are that lightning alone cannot provide better estimates than IR alone, but combining the two observations provides superior results to those obtained using any single sensor. Note that these results are not just a simple consequence of the calibration, because, even if we calibrate only the IR or only the lightning it does not yield better results than do the two combined. There is no significant difference among the algorithms in terms of bias. The

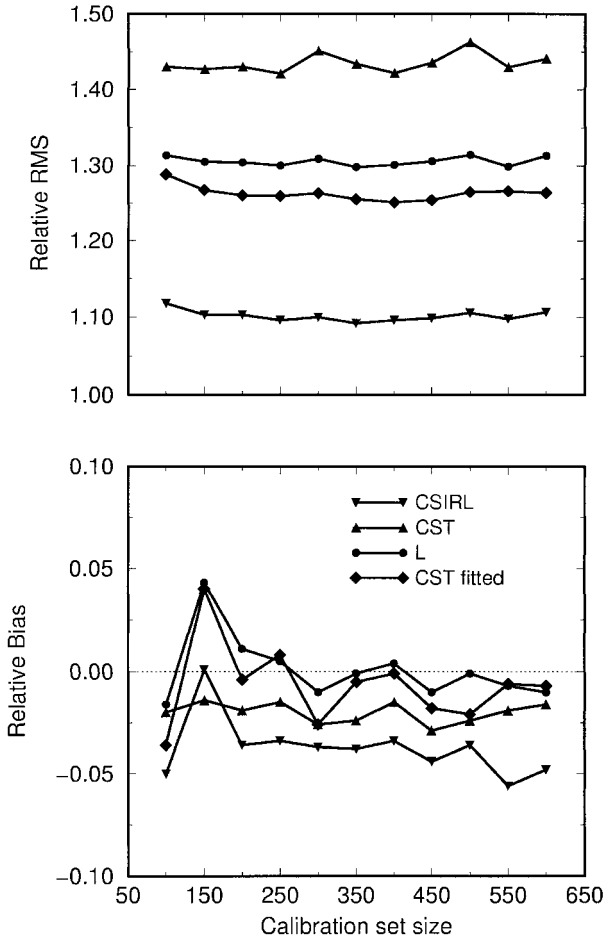

FIG. 7. Normalized rmse (top panel) and bias (bottom panel) vs the calibration dataset size.

bias is very low for all algorithms (within 5% of the SSM/I mean).

The analysis performed in the previous section indicates that CSIRL provides a 30% rmse reduction, with respect to the CST, in estimating the rain volume of convective cells with lightning activity. It was shown that about half of that improvement (15% rmse reduction) is due to the combined use of IR and lightning information, and the other half is an effect of the calibration. An important limitation of this technique, however, is that only a portion (less than half) of the convective rain is associated with lightning for the dataset used in this study (see Fig. 3). This fact is because there are convective rain areas not associated with cloud-to-ground lightning, and there are convective areas larger than the areas covered with significant lightning. These convective areas also may have resulted from false classification of the microwave signal. Nevertheless, the fact that the cloud-to-ground lightning area and consequently the convective rain area defined by CSIRL are expected to underestimate the total convective area as indicated by satellite microwave data is important, and its consequence to the estimation of total rainfall will be assessed in the following section.

TABLE 1. Contingency scores for lightning vs convective rain occurrences.

POD	FAR	CSI
0.36	0.35	0.30

To characterize statistically the agreement between satellite microwave (SSM/I) and NLDN lightning observations, we used three performance scores: the probability of detection (POD), the false alarm rate (FAR), and the critical success index (CSI), defined as

$$\mathrm{POD} = \frac{n_{\mathrm{success}}}{n_{\mathrm{success}} + n_{\mathrm{failure}}}, \tag{3}$$

$$\mathrm{FAR} = \frac{n_{\mathrm{false\ alarm}}}{n_{\mathrm{success}} + n_{\mathrm{false\ alarm}}}, \quad \text{and} \tag{4}$$

$$\mathrm{CSI} = \frac{n_{\mathrm{success}}}{n_{\mathrm{success}} + n_{\mathrm{failure}} + n_{\mathrm{false\ alarm}}}, \tag{5}$$

where n_{success}, n_{failure}, and $n_{\mathrm{false\ alarm}}$ are the numbers of successes, failures, and false alarms, respectively, in the comparison. A comparison yields a success when there is lightning and a GPROF (SSM/I) rainfall rate greater than 8 mm h^{-1}, a false alarm when there is lightning but not rainfall, and a failure when there is rainfall greater than 8 mm h^{-1} with no lightning indications. We chose the threshold of 8 mm h^{-1} because the histogram in Fig. 1 shows a significant decrease in convective rainfall occurrence below this value. Our criterion defining the false alarm is relaxed because classification of low rainfall rates from microwave data can be uncertain (Anagnostou and Kummerow 1997). We considered that the threshold-based evaluation, with the relaxed definition of a false alarm, is less sensitive to regime classification errors, because it does not penalize the errors for pixels with relatively low rainfall rates ($<$8 mm h^{-1}). The results are given in Table 1. The scores are inferior to those found by Tappia et al. (1998), but this inferiority mainly is due to resolution differences (12 km $\times$ 12 km vs 1 km $\times$ 1 km) and the higher uncertainty in satellite–microwave- versus radar-based classification. The percentages indicated in Figs. 1 and 3 qualitatively agree with the scores given in Table 1.

The CSIRL convective parameterization is demonstrated to be superior to single-sensor retrievals in estimating rainfall volume within the convective areas defined by lightning clusters. It is important, however, to understand how relevant the information on the convective contribution to the total rainfall, derived from lightning data, can be for the overall accuracy of any convective–stratiform precipitation estimation technique. This subject is approached next.

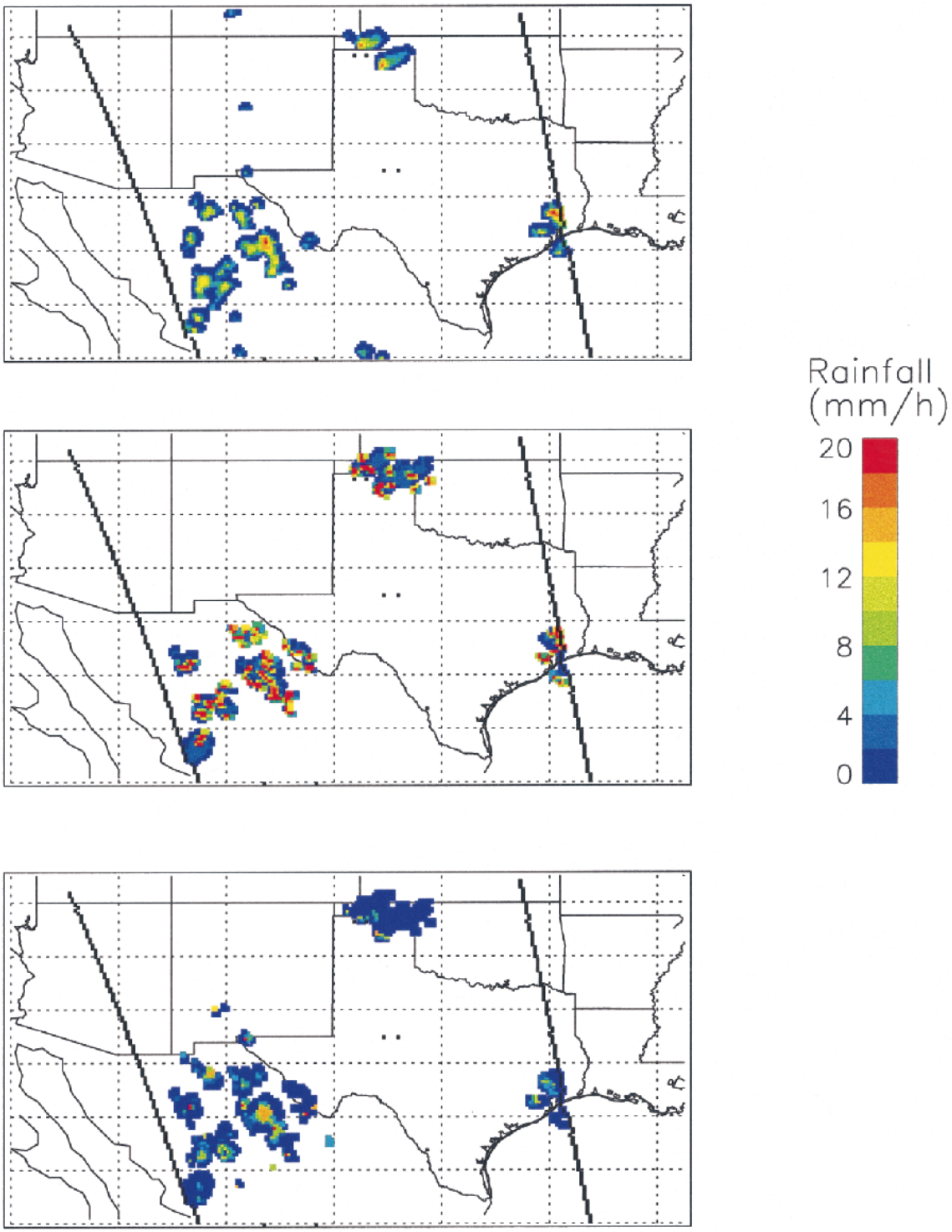

FIG. 8. (top panel) GPROF-based, (middle panel) CST-based, and (bottom panel) combined IR–lightning-based rain estimates, 15 Jul 0014 UTC.

5. Examples and evaluation of a full CSIRL technique

As discussed above, the CSIRL parameterization concerns only the estimation of the convective rainfall volume within clusters defined by lightning strikes. The assumption is made that the total convective precipitation portion of the storm is confined within the defined lightning clusters. The lightning-free areas in the cloud

are assumed to be either rain free or stratiform precipitation regions. The stratiform precipitation regions are derived from IR data using a technique similar to CST. These stratiform precipitation areas are assigned a constant rainfall rate equal to the mean stratiform rainfall as indicated by the SSM/I-based classification. This value is 3.76 mm h^{-1} for the dataset used in the study. This way is not necessarily the best way to treat nonlightning situations, given that there might be convective cells with no lightning indications (see Fig. 2). Alternative ways may be to incorporate information on minima in the IR array and its local spatial variability (Anagnostou et al. 1999). In the following, we present intercomparisons between microwave instantaneous rainfall and rainfall retrieved from the combined IR–lightning technique (hereinafter called full CSIRL) and IR-only CST.

Examples of three rainfall estimates derived from 1) SSM/I (GPROF), 2) IR-only (CST) and 3) the full CSIRL are shown in Fig. 8. Notice that the CST estimates show an unnaturally large spatial variability, which might be an effect of the crisp convective–stratiform classification. The combined lightning and IR estimates do not exhibit this behavior, because the disaggregation of the clusters' rain volume is made according to the spatial distribution of the IR temperatures, which is characterized by smooth gradients. One can observe that, even at the level of rainfall maps, combinations of lightning and IR can provide rain patterns much closer to SSM/I rainfall than can IR alone. This hypothesis is difficult test comprehensively at high spatial resolutions (e.g., 12-km pixel size) because of uncertainties associated with the spatial and temporal mismatches between the different sensors. With a sufficiently large dataset, which can provide a calibration and validation without requiring successive resampling, testing of this hypothesis may be feasible.

The rainfall histograms of CST, full CSIRL, and GPROF presented in Fig. 9 illustrate problems associated with each type of estimate. The CST histogram is bimodal because of the strong dependence of the rainfall–temperature relationship on classification. The full-CSIRL estimates exhibit a long-tailed distribution that is most likely a calibration effect, which is made at the level of clusters.

Figures 8 and 9 contain qualitative information about the full-CSIRL performance. As stated at the beginning of this section, the full-CSIRL performance is expected to be different from its convective parameterization (CSIRL) rainfall estimation performance. Consequently, we calculated the full-CSIRL and CST overall rmse and differential bias against the GPROF (SSM/I) estimates. For reasons discussed before, we calculated the error statistics for larger areas and not at the level of individual pixels. The aggregation areas (rain clusters) were defined by the 235-K isotherm in the IR temperature array. In this way, we defined 2856 clusters with areas ranging from 144 to 119 952 km^2. For each cluster, rainfall volumes were calculated using the CST and full-CSIRL techniques. The corresponding reference rainfall volumes were derived from SSM/I data using GPROF. The clusters' rmse and bias were calculated conditionally on selected rain volume thresholds.

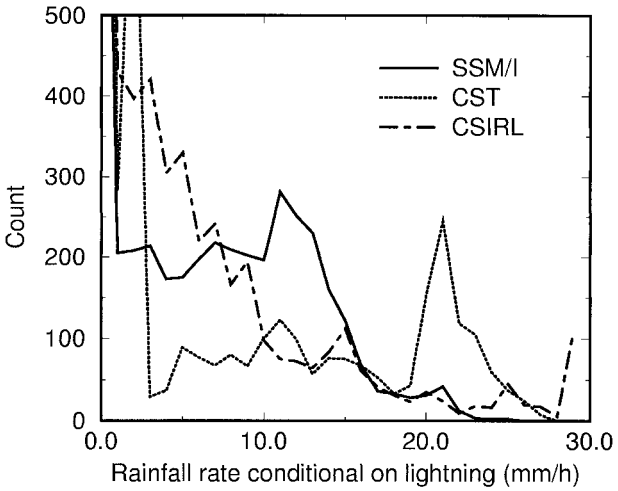

FIG. 9. Plots of the CST, CSIRL, and GPROF rainfall estimates at 12-km pixels with lightning occurrences.

The results for five different thresholds are presented in Fig. 10. We may make several observations based on this error analysis. There is a 17% rmse reduction for the zero-rain threshold (all clusters included), for which also the full-CSIRL bias is smaller than the CST bias. Only for the threshold of 5 mm h^{-1} does full CSIRL have slightly worse error statistics than CST does. For large thresholds, full CSIRL's error statistics are significantly smaller than are CST's error statistics. Results are consistent with Negri and Adler's (1993) observation that CST may wrongly identify large stratiform regions as convective but also misinterpret some of the convective rain as stratiform.

Additional information concerning the performance of full CSIRL versus CST is given in Table 2. We calculated the POD, FAR, and CSI scores as follows. For a certain rain threshold, success was considered when the estimated (i.e., full CSIRL or CST) and reference (GPROF) rainfall rates were greater than the threshold. A failure was considered when the reference rain was greater than the threshold, and the corresponding estimate was smaller. A false alarm occurred when the estimate was greater than the threshold, and the reference was smaller. One may observe that, for small thresholds (0 and 2 mm h^{-1}), full CSIRL performed better than CST did, especially in the POD score. The higher POD indicates the utility of the lightning method in detecting precipitating areas that are missed by CST. For moderate rainfall thresholds (5 and 10 mm h^{-1}), CSIRL performance in terms of detection decreases. This decrease is because some of the convective rain may not be associated with lightning and because the full-CSIRL estimates are spatially smooth as a consequence of the al-

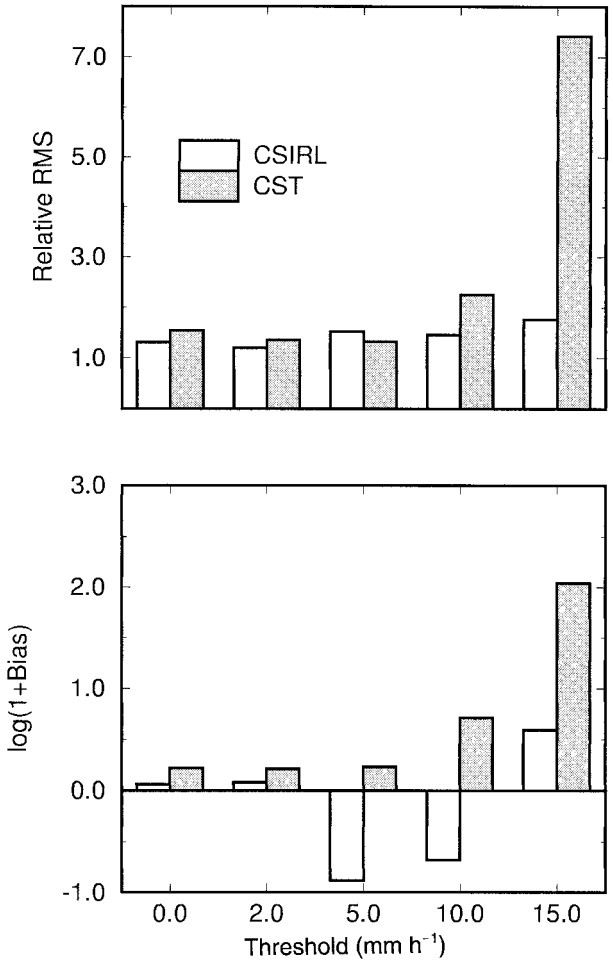

FIG. 10. (top panel) Normalized rmse and (bottom panel) bias vs rainfall rate threshold.

location technique. At high rainfall thresholds (15 mm h^{-1}), CST has higher POD than does full CSIRL but also has a very high FAR that yields a smaller CSI than that of full CSIRL. This result is consistent with Fig. 10, which indicates large overestimation by CST of high rainfall rates.

6. Conclusions

The general conclusion of this study is that lightning data contain useful information for IR rainfall estimation. Results show a reduction of about 15% in the rms of the estimates of rain volumes defined by lightning clusters. Moreover, the benefits of using lightning data in rainfall estimation are not limited only to convective rain associated with lightning. We demonstrated that the error caused by missing convective rain areas because of the absence of lightning is smaller than the error caused by overestimating the convective rain areas using IR-only data.

We consider that the improvement in results could have been even more significant, but several artifacts such as uncertainty in SSM/I rainfall products and their coarse spatial resolution prevented us from demonstrating it. Although, at larger scales, the improvement of using the CSIRL algorithm is obvious, it diminishes as the scale decreases. That fact may be because the allocation of the cluster's rainfall volume to each particular pixel, based on the IR frequency histogram, is not the most rigorous approach. Also errors in collocating the satellite microwave convective areas and lightning positions negatively affect the CSIRL performance. Better alternatives for estimating large-area convective rain and distributing it to individual pixels need to be investigated. Investigating these alternatives may not be possible unless higher-resolution data that allow a better identification of the convective areas and lightning positions are used. Higher-resolution data, such as radar data, would reduce the scale of aggregation and, consequently, the necessity of disaggregation and its effect on estimation. Also, for rain estimation in the areas not characterized by lightning, newly developed and potentially better algorithms than CST (e.g., Anagnostou et al. 1999) may be considered. Further research is needed to consider these issues to provide more comprehensive evidence concerning the potential of lightning in rainfall estimation.

TABLE 2. Contingency scores for conditional rainfall rate estimates.

Threshold (mm h^{-1})	CSTL			CST		
	POD	FAR	CSI	POD	FAR	CSI
0.0	0.65	0.48	0.41	0.56	0.48	0.37
2.0	0.64	0.47	0.29	0.32	0.62	0.23
5.0	0.20	0.38	0.18	0.34	0.59	0.23
10.0	0.15	0.61	0.11	0.32	0.78	0.15
15.0	0.18	0.87	0.08	0.31	0.95	0.04

Acknowledgments. This research was initiated at NASA's Goddard Space Flight Center while Dr. Mircea Grecu was a USRA Graduate Student Summer Program participant. The authors gratefully acknowledge insightful discussions and helpful data compilation support by Mr. Carlos A. Morales of the University of Connecticut. The NLDN data were provided by NASA DAAC/MSFC, and the GOES data were provided by Dennis Chesters of GSFC/NASA. Financial support for this research was provided by NASA's New Investigator Program grant awarded to Dr. Emmanouil N. Anagnostou.

REFERENCES

Adler, R. F., and A. J. Negri, 1988: A satellite infrared technique to estimate tropical convective and stratiform rainfall. *J. Appl. Meteor.*, **27,** 30–51.

Alexander, G. D., J. A. Weinman, V. M. Karyampudi, W. S. Olson, and A. C. L. Lee, 1999: The effect of assimilating rain rates derived from satellites and lightning on forecasts of the 1993 superstorm. *Mon. Wea. Rev.*, **127,** 1433–1457.

Anagnostou, E. N., and C. Kummerow, 1997: Stratiform and convective classification of rainfall using SSM/I 85-GHz brightness temperature observations. *J. Atmos. Oceanic Technol.,* **14,** 570–575.

——, A. J. Negri, and R. F. Adler, 1999: A satellite infrared technique for diurnal rainfall variability studies. *J. Geophys. Res.* (*Atmos.*), **104,** 31 477–31 488.

Cheze, J. L., and H. Sauvageot, 1997: Area-average rainfall and lightning activity. *J. Geophys. Res.,* **102,** 1707–1715.

Conner, M. D., and G. Petty, 1998: Validation and intercomparison of SSM/I rain-rate retrieval over the continental United States. *J. Appl. Meteor.,* **37,** 679–700.

Goodman, S. J., 1990: Predicting thunderstorm evolution using ground-based lightning detection networks. NASA Tech. Memo. TM-103521, 210 pp.

——, D. Buechler, and P. J. Meyer, 1988: Convective tendency images derived from a combination of lightning and satellite data. *Wea. Forecasting,* **3,** 173–188.

Kummerow, C., 1998: Beamfilling errors in passive microwave rainfall retrievals. *J. Appl. Meteor.,* **37,** 356–370.

——, W. S. Olson, and L. Giglio, 1996: A simplified scheme for obtaining hydrometeor profiles from passive microwave sensors. *IEEE Trans. Geosci. Remote Sens.,* **34,** 1213–1232.

MacGorman, D. R., and C. D. Morgenstern, 1998: Some characteristics of cloud-to-ground lightning in mesoscale convective systems. *J. Geophys. Res,* **103,** 14 011–14 023.

Mackerras, D., M. Darveniza, R. E. Orville, E. R. Williams, and S. J. Goodman, 1998: Global lightning: Total, cloud and ground flash estimates. *J. Geophys. Res.,* **103,** 19 791–19 809.

Maddox, R. A., H. W. Howard, and C. L. Dempsey, 1997: Intense convective storms with little or no lightning over central Arizona: A case of inadvertent weather modification? *J. Appl. Meteor.,* **36,** 302–314.

Morales, C. A. R., J. A. Weinman, and J. S. Kriz, 1998: Continuous monitoring of convective rainfall derived from combined spaceborne microwave, IR and ground based sferics measurements. *Proc. IGARS,* Vol. 3, Seattle, WA, The Institute of Electrical and Electronics Engineers, 1683–1685.

Negri, A. J., and R. F. Adler, 1993: An intercomparison of three satellite infrared rainfall techniques over Japan and surrounding waters. *J. Appl. Meteor.,* **32,** 357–373.

Noreen, E. W., 1989: *Computer-Intensive Methods for Testing Hypotheses: An Introduction.* John Wiley and Sons, 229 pp.

Petersen, W. A., and S. A. Rutledge, 1998: On the relationship between cloud-to-ground lightning and convective rainfall. *J. Geophys. Res.,* **103,** 14 025–14 040.

Sheridan, S. C., J. F. Griffiths, and R. E. Orville, 1997: Warm season cloud-to-ground lightning–precipitation relationships in the south-central United States. *Wea. Forecasting,* **12,** 449–457.

Steiner, M., R. A. Houze Jr., and S. E. Yuter, 1995: Climatological characterization of three-dimensional storm structure from operational radar and rain gauge data. *J. Appl. Meteor.,* **34,** 1978–2007.

Tappia, A., J. A. Smith, and M. Dixon, 1998: Estimation of convective rainfall from lightning observations. *J. Appl. Meteor.,* **37,** 1497–1509.

Toracinta, E. R., K. I. Mohr, E. J. Zipser, and R. E. Orville, 1996: A comparison of WSR-88D reflectivities, SSM/I brightness temperatures, and lightning for mesoscale convective systems in Texas. Part I: Radar reflectivity and lightning. *J. Appl. Meteor.,* **35,** 902–918.

Zipser, E. J., 1994: Deep cumulonimbus cloud systems in the Tropics with and without lightning. *Mon. Wea. Rev.,* **122,** 1837–1851.